

# Short-Period Planetary Waves in the Antarctic Middle Atmosphere

A. J. G. Baumgaertner<sup>a</sup>, A. J. McDonald<sup>b</sup>, R. E. Hibbins<sup>c</sup>,  
D. C. Fritts<sup>d</sup>, D. J. Murphy<sup>e</sup>, R. A. Vincent<sup>f</sup>

<sup>a</sup>*Department of Physics and Astronomy, University of Canterbury, Christchurch  
8020, New Zealand. Now at: Max Planck Institute for Chemistry, Postfach 30 60,  
55020 Mainz, Germany.*

<sup>b</sup>*Department of Physics and Astronomy, University of Canterbury, Christchurch  
8020, New Zealand.*

<sup>c</sup>*Physical Sciences Division, British Antarctic Survey, Cambridge CB3 0ET, UK.*

<sup>d</sup>*NorthWest Research Associates/Colorado Research Associates Division, CO,  
USA.*

<sup>e</sup>*Australian Antarctic Division, 203 Channel Highway, Kingston, Tasmania, 7050,  
Australia.*

<sup>f</sup>*The University of Adelaide, Adelaide SA, 5005, Australia.*

---

**Abstract**

1 Planetary waves with periods between two and four days in the middle atmosphere  
2 over Antarctica are characterized using one year of data from the medium-frequency  
3 spaced antenna (MFSA) radars at Scott Base, Rothera and Davis. In order to inves-  
4 tigate the origin of the observed waves, the ground based data are complemented by  
5 temperature measurements from the EOS MLS instrument on the Aura satellite as  
6 well as wind velocity data from the UKMO stratospheric assimilation. Observations  
7 of waves with a period of approximately two days in summer are consistent with  
8 the quasi-two-day wave (QTDW) generally found after the summer solstice at low-  
9 and mid-latitudes. The Scott Base observations of the QTDW presented here are  
10 the highest-latitude ground based observations of this wave to date. Winter waves  
11 with preferred periods of two and four days occur in bursts throughout the win-  
12 ter with maximum activity in June, July, and August. The mean of the two and  
13 four day wave amplitudes is relatively constant, suggesting constant wave forcing.  
14 When several waves with different periods occur at the same time, they often have  
15 similar phase velocities, supporting suggestions that they are quasi-non-dispersive.  
16 In 2005, a “warmpool” lasts from late July to late August. Exploring the role of  
17 vertical shear (baroclinic instabilities) and horizontal shear (barotropic instabilities)  
18 of the zonal wind suggests that instabilities are likely to play a role in the forcing of  
19 the two-day and four-day waves, which are near-resonant modes and thus supported  
20 by the atmosphere.

*Key words:* MFSA radar, QTDW, MLS, baroclinic and barotropic instabilities

---

---

*Email address:* [abaumg@mpch-mainz.mpg.de](mailto:abaumg@mpch-mainz.mpg.de) (A. J. G. Baumgaertner).

## 21 1 Introduction

22 Planetary waves play an important role in the global circulation (Salby, 1984;  
23 Andrews et al., 1987; Volland, 1988). The quasi-two-day wave (QTDW) often  
24 dominates the wind field in the middle atmosphere at low- and mid-latitudes  
25 during summer, and waves with periods of two to four days are prominent at  
26 high latitudes during winter. Because of their prominence, waves with periods  
27 between two and four days have received a great deal of attention over the  
28 last 35 years. A wind oscillation with a period of approximately 51 hours was  
29 described for the first time by Muller (1972) during July and August in the up-  
30 per mesosphere at 53°N. This study was followed by many other studies (e.g.  
31 Kalchenko and Bulgakov, 1973; Craig and Elford, 1981) that reported obser-  
32 vations of a similar phenomenon during the summer solstice in the northern  
33 and southern hemispheres. A main characteristic of all reports is the burst-  
34 like occurrence shortly after the solstice. Southern hemisphere data usually  
35 showed a period closer to 48 hours (Harris, 1994), but in the northern hemi-  
36 sphere the oscillation was reported to be longer than two days, with periods  
37 of up to 53 hours being observed. The wave was termed the quasi-two-day  
38 wave (QTDW) because its period varied with season and location. The wave  
39 has since been studied extensively using radar and satellite data, and mod-  
40 els. While at mid-latitudes the zonal and meridional components have similar  
41 amplitudes, the meridional wind component was found to dominate over the  
42 zonal component towards the equator. In general, the southern hemisphere  
43 wind amplitudes were observed to reach 50 m/s and are larger by a factor of  
44 about 2 compared with northern hemisphere observations where meridional  
45 amplitudes of 20 m/s were reported. Satellite studies using temperature data

46 from Nimbus 7 (Rodgers and Prata, 1981), UARS (Wu et al., 1993; Limpasu-  
47 van and Wu, 2003), TIMED (Garcia et al., 2005), and EOS Aura (Limpasuvan  
48 et al., 2005) show temperature amplitudes of up to 11 K in southern summers  
49 and weaker amplitudes in northern summers. The QTDW was also detected in  
50 satellite measurements of water vapor (Limpasuvan and Wu, 2003) and wind  
51 (Wu et al., 1993; Limpasuvan et al., 2005).

52 Soon after the discovery of the oscillation, studies of the zonal structure of the  
53 wave followed. Radar as well as satellite measurements have now established  
54 that the wave has a westward propagating zonal wavenumber 3 structure in  
55 both hemispheres (e.g. Glass et al., 1975; Wu et al., 1993), sometimes mixed  
56 with other modes of wavenumber 4 (Meek et al., 1996).

57 The origin of the QTDW has been discussed widely. Salby (1981) reviewed the  
58 middle atmosphere QTDW observations and showed that a wave with a pe-  
59 riod near 2.1 days and zonal wavenumber 3 structure is a resonant Eigenmode,  
60 called a Rossby-gravity normal mode, in a windless isothermal atmosphere. In  
61 more realistic wind fields, the mode's period was approximately 2.22 days dur-  
62 ing the solstice and showed features very similar to those observed. Although  
63 characteristics of the Rossby-gravity wave mode depend on the background  
64 wind, this was not seen as a sufficient explanation of the burst-like behavior  
65 of the QTDW and hence an alternative explanation was proposed by Plumb  
66 (1983). Plumb (1983) investigated whether the strong wind velocity gradients  
67 at the edge of the mesospheric summer jet could create instabilities that could  
68 generate the QTDW. A one-dimensional instability analysis showed that if  
69 the vertical shear in the jet is large enough, the jet becomes baroclinically  
70 unstable and creates a wave with properties similar to those observed. Pfister  
71 (1985) obtained similar results for wind amplitudes with a two-dimensional

72 quasi-geostrophic model, but temperature and geopotential maxima occurred  
73 at middle to high latitudes which does not agree with observations. The in-  
74 stability theory was supported by studies of the meridional gradient of quasi-  
75 geostrophic potential vorticity in the NMC reanalysis data set (Randel, 1994),  
76 in general circulation models (Norton and Thuburn, 1996), and in radar and  
77 UARS HRDI data (Fritts et al., 1999).

78 During winter, a QTDW has also been identified in the stratosphere and meso-  
79 sphere. However, it appears to be connected to waves with periods between  
80 1.7 and 4 days or even longer which are now reviewed briefly. Waves in this  
81 period range were described for the first time by Venne and Stanford (1979)  
82 using satellite measurements and were found to have eastward phase velocities.  
83 Because of rapid growth with height and small vertical phase variations, the  
84 waves were concluded to be forced in situ. Instability analysis using observa-  
85 tional data and models showed that barotropic and/or baroclinic instabilities  
86 of the polar night jet can generate the observed waves (Charney and Stern,  
87 1962; Hartmann, 1983; Manney et al., 1988; Randel and Lait, 1991; Manney,  
88 1991; Palo et al., 1998), similar to QTDW generation by the summer meso-  
89 sphere jet proposed by Plumb (1983). Waves with periods between two and  
90 four days in the Antarctic mesosphere were described by Fraser et al. (1993)  
91 and found to be consistent with barotropic instability studies. Very recently,  
92 Murphy et al. (2007) discussed a climatology of wave activity from Davis  
93 (69°S) employing data from the MFSA radar that is also used for the present  
94 study, and OH temperature measurements. The study revealed wave activity  
95 in the 1.7-4 day period band occurring throughout the year, with minima at  
96 the equinoxes. The authors attributed most of the activity in this band to the  
97 QTDW. In the northern polar winter mesosphere a QTDW was reported by

98 Nozawa et al. (2003a). Nozawa et al. (2003a) used wind measurements from  
99 an MFSA radar at Tromsø (70°N) and found that the amplitude maximises  
100 between 70 and 82 km near winter solstice. Later Nozawa et al. (2003b) con-  
101 firmed these findings using data from MFSA radars at Tromsø (70°N) and  
102 Poker Flat (65°N).

103 Seasonal variations of the QTDW corresponded closely between the two sites,  
104 but variations on shorter time-scales were not synchronized well. Nozawa et al.  
105 (2003b) reported that the zonal wavenumber appeared to be 2 or 4 more often  
106 than 3; moreover, the possibility that the wave propagates eastward was con-  
107 sidered. A winter QTDW has also been observed at Saskatoon (52°N) using  
108 MFSA radar data (Chshyolkova et al., 2005). Similar to the studies by Nozawa  
109 et al., the wave’s amplitude was reported to maximise at lower altitudes (ap-  
110 proximately 70 km) than the summer QTDW (85–88 km). Lawrence et al.  
111 (1995) used radar observations together with stratospheric analyses to show  
112 that a 4-day wave can reach to the Antarctic upper mesosphere. The study  
113 confirmed that the wave is associated with quasi-nondispersive warm pools  
114 that rotate in the polar vortex.

115 In the present work, waves with periods between two and four days observed  
116 over the southern polar regions during summer and winter are characterized  
117 using MFSA radars at Scott Base, Rothera and Davis. The ground based data  
118 are complemented by EOS MLS satellite data and the UKMO stratospheric  
119 assimilation to investigate the origins of the planetary waves.

Station	transmitted frequency	pulse width (FWHM)	sampling frequency	reference
Scott Base	2.9 MHz	30 $\mu$ s	2 min	Baumgaertner et al. (2005)
Rothera	1.98 MHz	25 $\mu$ s	2 min	Jarvis et al. (1999)
Davis	1.94 MHz	30 $\mu$ s	2 min	Murphy (2002)

Table 1

Overview of employed MF radars

## 120 2 Data and Analysis Techniques

121 Horizontal wind velocity data from the MFSA radars at Scott Base (78°S,  
122 167°E), Davis (69°S, 78°E), and Rothera (68°S, 68°W) are employed. The  
123 measurements are based on the correlation analysis of moving diffraction pat-  
124 terns of partial reflections from the mesosphere and lower thermosphere. The  
125 characteristics of the three radars are summarized in Table 1.

126 In addition to these ground-based instruments, temperature measurements  
127 from the Earth Observing System Microwave Limb Sounder (EOS MLS) on  
128 the Aura satellite are used. Microwave limb sounding uses thermal emissions  
129 with wavelengths in the millimeter and sub-millimeter region to infer atmo-  
130 spheric parameters. Measurements can be made day and night with a high  
131 vertical resolution. Aura was launched on 15 July 2004 into a sun-synchronous  
132 orbit with an inclination of 98° (a retrograde orbit) to 705 km altitude and flies  
133 in formation with the “A-Train”, a collection of several other Earth observa-  
134 tion satellites. The satellite orbits the Earth every 100 minutes and performs  
135 240 scans per orbit. EOS MLS measurements cover 82°N to 82°S every orbit

136 and yield concentrations of various constituents as well as temperature. Tem-  
137 peratures between 316 and 0.001 hPa are obtained from radiance measure-  
138 ments of O<sub>2</sub> at 118 GHz. The vertical resolution of the temperature product  
139 decreases throughout the stratosphere and mesosphere, starting at 4 km and  
140 decreasing to 9 km at 0.1 hPa. The first published validation study by Froide-  
141 vaux et al. (2006) states precisions of 0.5 K to 2 K and reports a warm bias of  
142 between 1 and 2 K when compared with other satellite and balloon measure-  
143 ments in the stratosphere. Version 1.51 of the EOS MLS data are employed  
144 in the present study.

145 Zonal wind velocities from the United Kingdom Met. Office (UKMO) strato-  
146 spheric assimilation are also presented here. The forecast model at the heart  
147 of the UKMO assimilation is the Met. Office Unified Model. For the strato-  
148 sphere, the assimilation incorporates data from the NOAA polar orbiters and  
149 radiosonde soundings. 50 model levels are available up to 0.1 hPa. In the hori-  
150 zontal, the data fields have a resolution of 2.5° latitude by 3.75° longitude. The  
151 Met. Office states horizontal wind RMS errors of 6.0 m/s at 100 hPa, 8 m/s  
152 at 10 hPa, and 12 m/s at 1 hPa. More details on the middle atmosphere data  
153 quality can be found in Swinbank et al. (1998).

154 Data are available from the MLS instrument for every day in 2005 except for  
155 10 days which are randomly distributed throughout the year. A strong solar  
156 proton event (SPE) in January caused total reflection of the medium frequency  
157 signal and thus no data are available from Davis and Scott Base during this  
158 period. The Rothera radar was not in operation for one week in February.  
159 The radar at Scott Base was not operational for several periods during the  
160 2005 winter due to technical problems. Other gaps in the radar data sets are  
161 confined to limited altitude regions and are due to low signal-to-noise ratios.

162 The year 2005 is the only year for which data from all three radars and the  
163 MLS instrument are available, therefore the present study discusses only a  
164 single year. In order to discuss climatological features, longer data sets would  
165 be necessary. However, this is beyond the scope of the present study.

### 166 **3 Results and Discussion**

#### 167 *3.1 Wave activity in summer*

168 A spectral analysis of the Scott Base, Davis, and Rothera MFSA observations  
169 is performed in order to determine the level of wave activity in the range of pe-  
170 riods between two and four days. Figure 1 depicts a running periodogram for  
171 each of the three radars obtained by fitting oscillations in the desired period  
172 band to the zonal wind velocities at 90 km for the year 2005. In order to detect  
173 waves with rapidly changing amplitudes and phases, intervals of 10 days were  
174 chosen and the rectangular window was shifted by 1 day increments through  
175 the entire year. White areas denote times when no data are available. It should  
176 be noted that the period axes have a logarithmic scale. A distinct feature at  
177 all three sites are the diurnal and semi-diurnal tides. Features of atmospheric  
178 tides at southern high latitudes are discussed in Baumgaertner et al. (2005)  
179 and references therein. Generally, there is a reasonable agreement of tidal  
180 amplitudes at the three stations, considering the latitudinal and longitudinal  
181 separation. At Rothera, tidal amplitudes appear smaller than at Scott Base  
182 and Davis, possibly due to interference of different tidal components (Baum-  
183 gaertner et al., 2006) or interactions with gravity waves (Fritts and Vincent,  
184 1987) since mountain waves have been found to enhance the gravity wave

185 field significantly in this area (Baumgaertner and McDonald, 2007). In early  
186 February oscillations with a period of approximately 2 days can be observed  
187 at the three sites, although at Davis the event is largest. The period lies be-  
188 tween 50 and 53 hours at all stations. Both the time of occurrence and the  
189 period indicate that this might be related to the QTDW observed at mid  
190 and low southern latitudes after summer solstice every year. In Figure 2 the  
191 periodograms for 80 km altitude are shown. Note that the amplitude of this  
192 QTDW event in February is smaller. Figure 3 depicts the mean amplitude  
193 in the range 2-4 days as a function of time and height for all three radars.  
194 Now the complete altitude range of the measurements can be surveyed and  
195 it is evident that the February QTDW wave event has maximum amplitudes  
196 between 85 and 90 km. This is consistent with other observations of the low-  
197 and mid-latitude QTDW (Chshyolkova et al., 2005) and other high latitude  
198 measurements (Murphy et al., 2007).

199 The relationship between the observed oscillation and the low- and mid-  
200 latitude QTDW can be further investigated by analysing the zonal structure  
201 of the wave, as the QTDW is most often found to be of wavenumber 3 or 4.  
202 The zonal wavenumber can be inferred using the phase differences of the wave  
203 between the three stations. Wavelet analysis is used to estimate the phases  
204 of the QTDW at the three stations. The commonly used Morlet function was  
205 employed here as a basis function. More details on the analysis method can be  
206 found in Torrence and Compo (1998). The wavelet analysis of the zonal wind  
207 at 90 km for Scott Base, Rothera and Davis is shown in Figure 4 for the period  
208 25 January to 9 February 2005. Note that the wavelet analysis was performed  
209 for a longer time series (1 January to 28 February 2005) than shown, so that  
210 the *cone of influence* falls outside the depicted interval. All three sites show

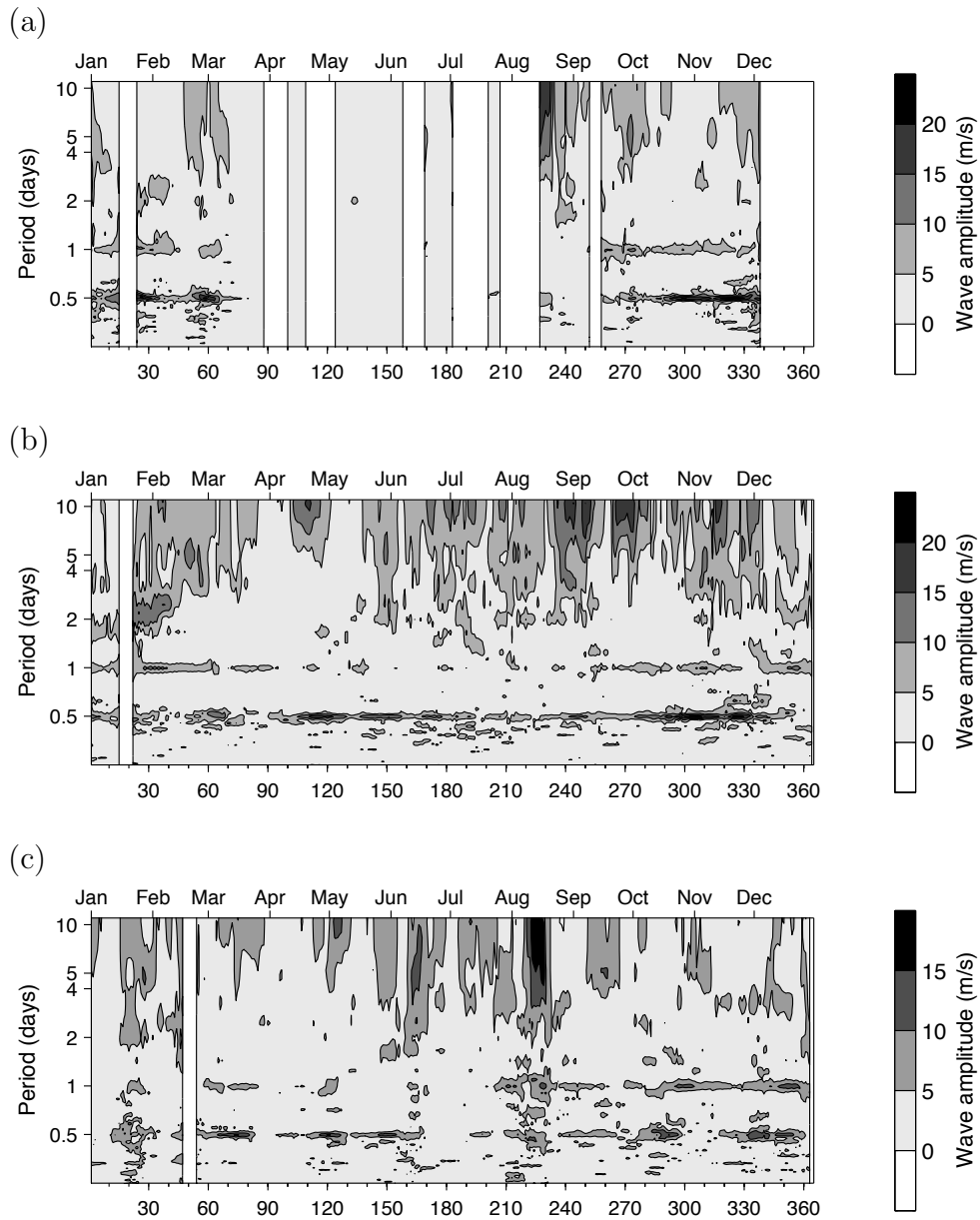


Fig. 1. Running periodograms of zonal wind velocities at Scott Base (a), Davis (b), and Rothera (c) at 90 km for the year 2005.

211 strong oscillations at approximately 51 hours, slightly longer than observed  
 212 elsewhere (Craig and Elford, 1981). They are weakest at Rothera, where the  
 213 wave is only clearly discernible from 28 January to 6 February, and strongest  
 214 at Davis. At Scott Base the QTDW is evident throughout the depicted pe-

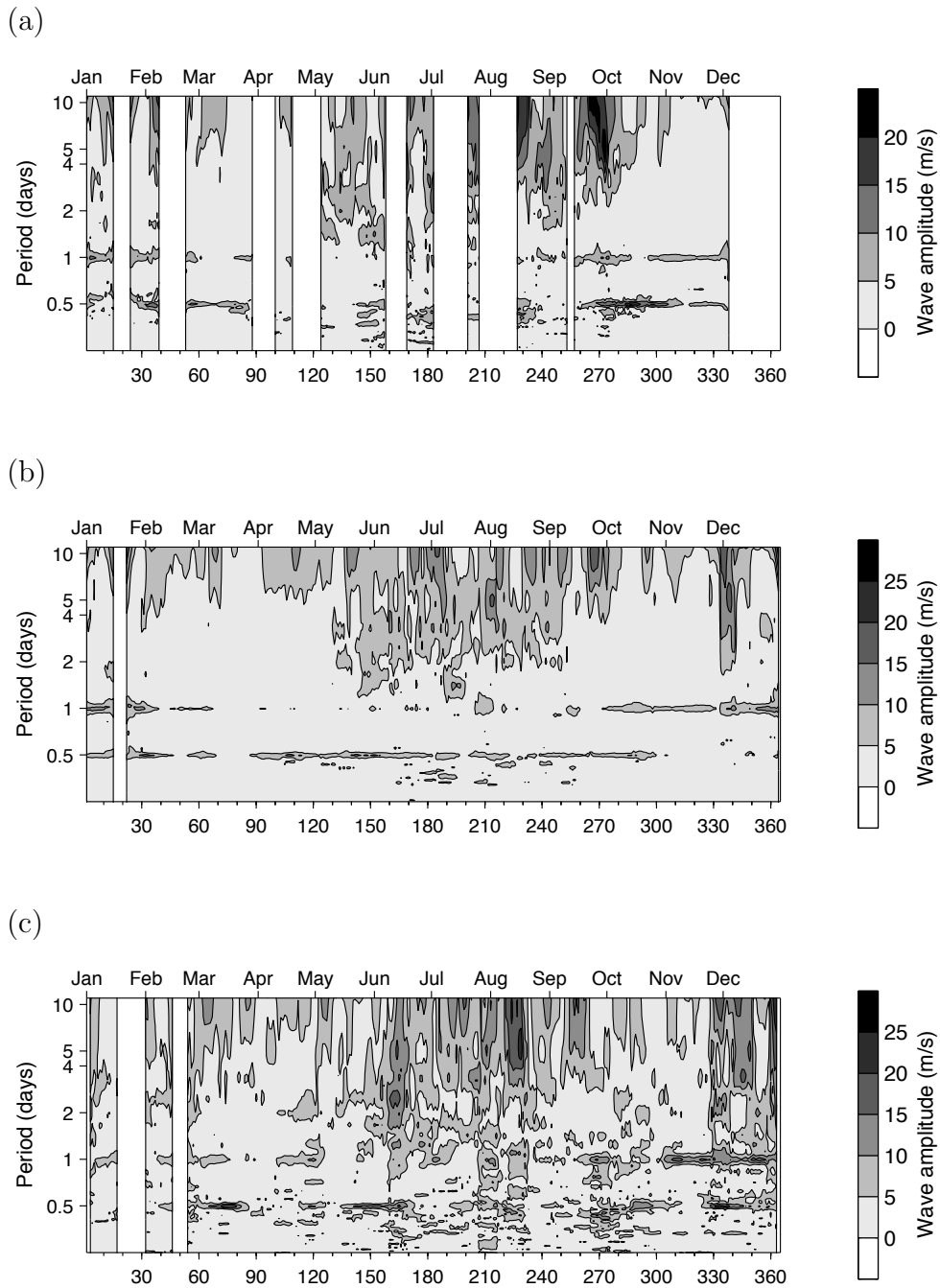


Fig. 2. Same as Figure 1 but for 80 km altitude.

215 riod, although it shows greater variability than at Davis. The time-series with  
 216 a period of 51 hours was extracted from the wavelet analysis. Then, a 51 hour  
 217 oscillation was fitted to rectangular 2-day windows of this time-series. This  
 218 yields the phase of the oscillation for each day and the phase differences be-

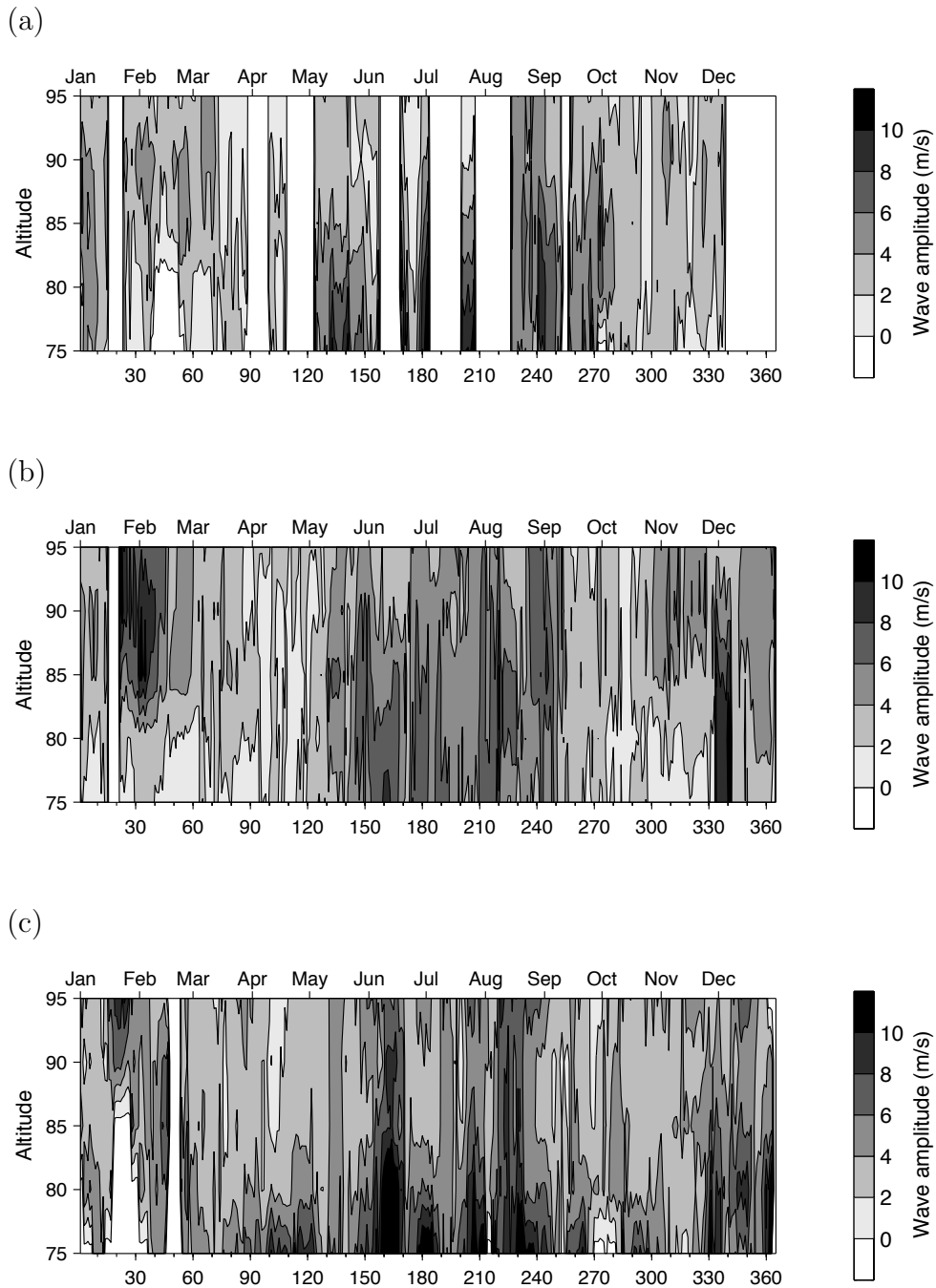


Fig. 3. Wave amplitude in the period range 2-4 days at Scott Base (a), Davis (b), and Rothera (c). White areas denote periods when no data are available.

219 tween all sites can then be calculated. The phase differences as a function of  
 220 time are depicted in Figure 5a for Rothera/Scott Base, in Figure 5b for Scott  
 221 Base/Davis, and in Figure 5c for Davis/Rothera. All phase differences are

222 shown assuming westward propagation of the wave as expected during sum-  
223 mer. It is also assumed that there is no phase change with latitude. The lines  
224 show the theoretical phase difference for pure wavenumber 1, 2, 3, and 4 waves  
225 calculated based on the longitudinal differences between the sites. All three  
226 pairs of stations indicate a reasonably good agreement with a wavenumber 3  
227 wave in both the zonal (crosses) and meridional (diamonds) wind measure-  
228 ments, the relationship being clearest in Figure 5b for the comparison between  
229 Scott Base and Davis observations. The discrepancies between the theoretical  
230 value and the measured phase differences are less than 5 hours in the zonal  
231 wind and less than 10 hours in the meridional wind on most days. Note that  
232 the differing phase differences on the last two days in Figure 5a are probably  
233 due to the low amplitude of the QTDW in the Rothera data (see Figure 4c),  
234 which leads to an inaccurate phase determination. Similarly, the fact that the  
235 amplitudes are smaller in the meridional than in the zonal direction is likely to  
236 be the reason for the larger discrepancies in the meridional phase differences.  
237 Overall this result suggests that the zonal structure of the wave observed at  
238 the three sites is a wavenumber 3 structure which further supports the hy-  
239 pothesis that the wave observed at these high latitude sites is associated with  
240 the low- and mid-latitude QTDW.

241 The wavenumber of waves observed in satellite temperature measurements can  
242 be easily obtained using wavenumber/frequency spectral analysis (Wu et al.,  
243 1995). This gives a more reliable estimate of the wavenumber and propagation  
244 direction than the limited ground-based measurements.

245 For spectral analysis of the MLS temperature data a least squares method is  
246 employed (Wu et al., 1995). Frequency,  $\sigma$ , and wavenumber,  $s$ , are found by

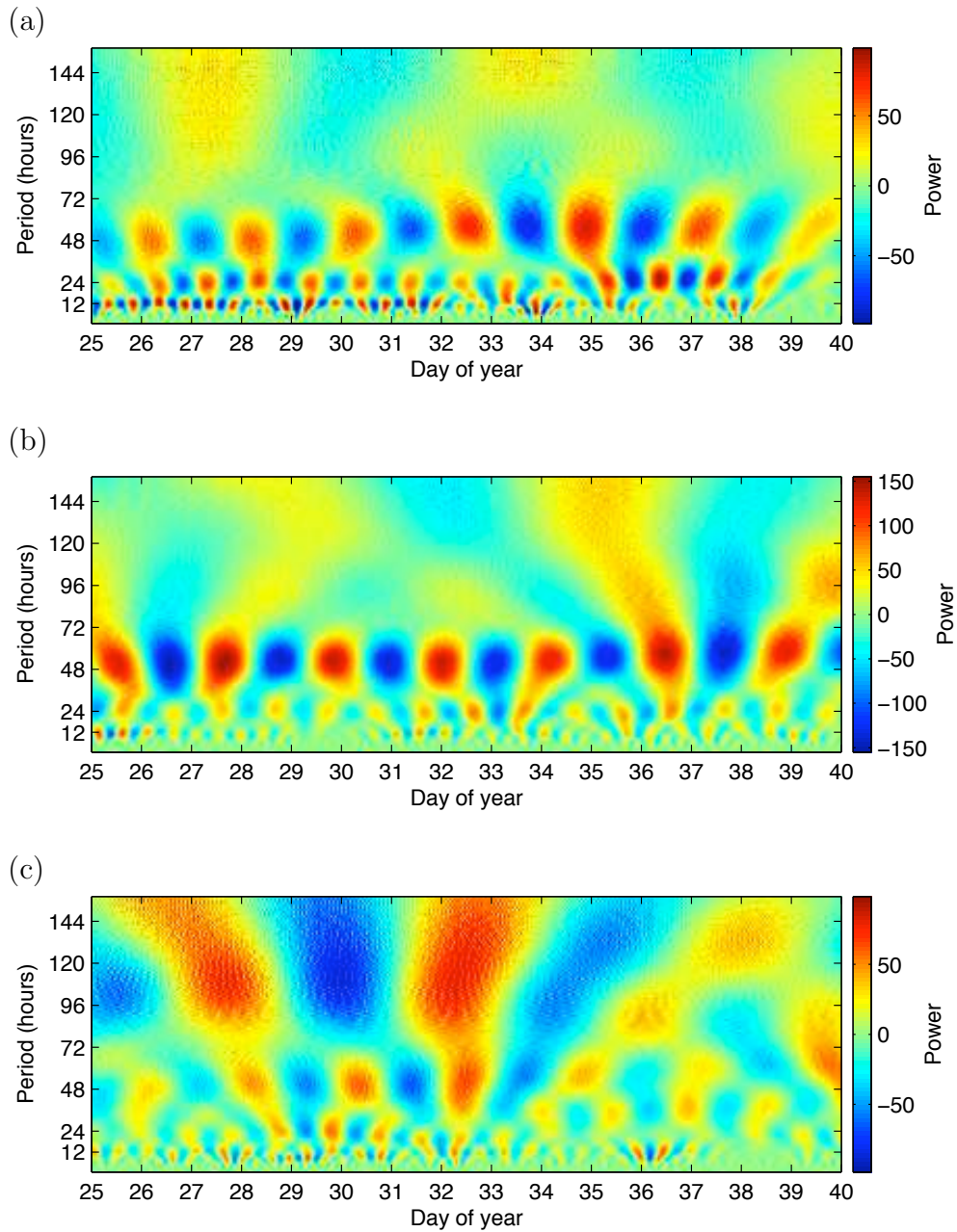


Fig. 4. Wavelet analysis of the zonal wind measured at Scott Base (a), Davis (b), and Rothera (c) for 25 January to 9 February 2005 at 90 km. Positive power indicates eastward velocities, negative power indicates westward velocities

247 fitting observations to a model of the form

$$248 \quad y_i = A \cos(2\pi(\sigma t_i + s\lambda_i)) + B \sin(2\pi(\sigma t_i + s\lambda_i)) \quad (1)$$

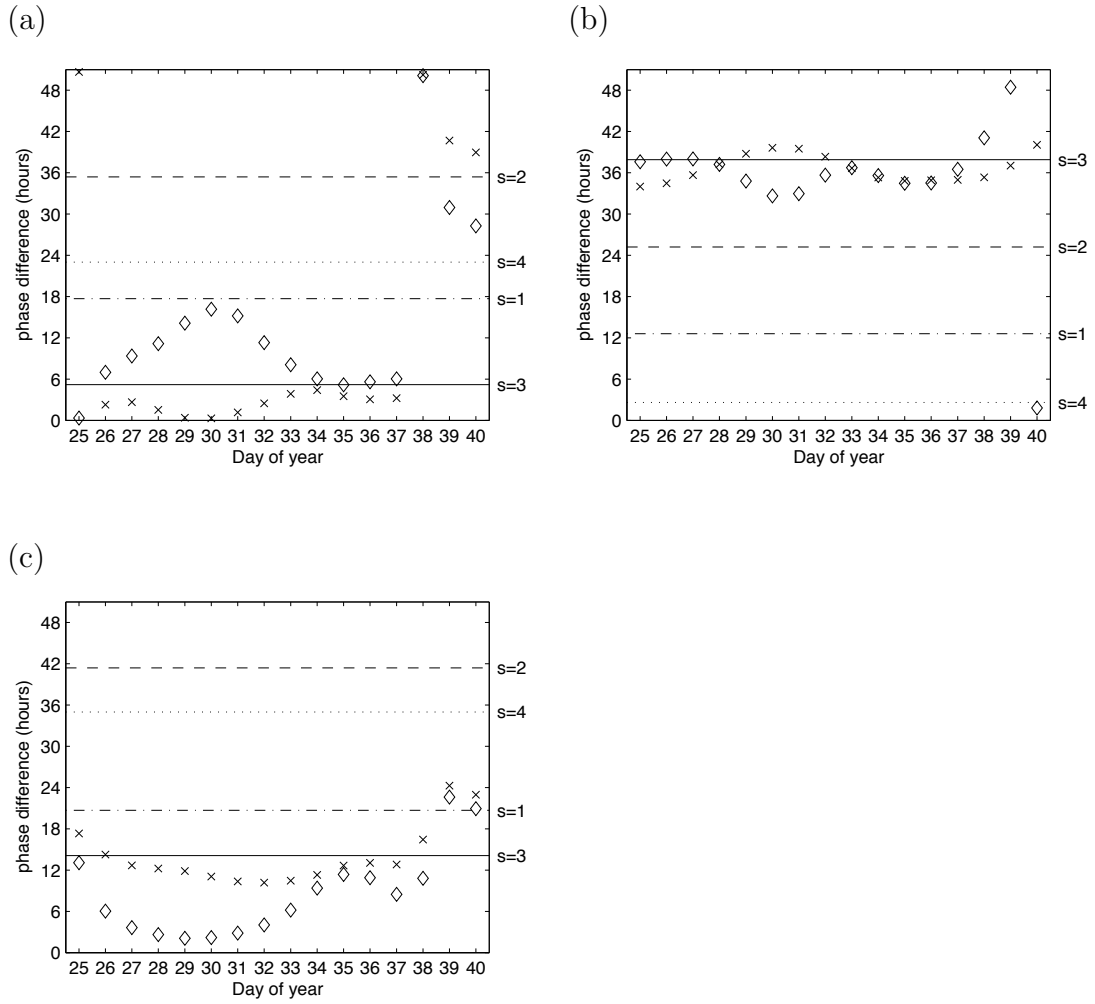


Fig. 5. Phase differences of the 51 hour wave between Rothera/Scott Base (a), Scott Base/Davis (b), and Davis/Rothera (c) for 25 January to 9 February 2005 at 90 km. Crosses: zonal wind, diamonds: meridional wind. Dash-dotted, dashed, Solid and dotted lines denote the expected phase differences for wavenumber 1, 2, 3, and 4, respectively, for the given longitudinal separations.

249 to the set of zero mean observations  $y_i$ .  $y_i$  are measured at  $t_i$  (days, in universal  
 250 time (UT)) and normalized longitude  $\lambda_i$ . For the present work we used a length  
 251 of 10 days for the fits, and incremented the window in steps of one day.

252 The analysis for 25 January to 9 February 2005 of MLS temperature at  
 253 0.005 hPa (approximately 86 km) using data at 70°S is depicted in Figure 6.

254 Only frequency/wavenumber pairs significant above the 95% level are dis-  
255 played. The strongest peak appears at frequency 0.45 cyc/d (53.3 hours) with  
256 wavenumber 3 (westward propagating). The spectral resolution of this analysis  
257 technique is given by (Wu et al., 1995):

$$258 \quad (\Delta\sigma T)^2 + (\Delta s)^2 = a^2, \quad (2)$$

259 where  $\Delta\sigma$  is the resolution in frequency,  $\Delta s$  is the resolution in wavenumber,  
260  $T$  is the total sample length and  $a$  is a constant for which values between 1  
261 and 1.45 have been recommended (Wu et al., 1995). For  $a = 1.2$ , in order to  
262 distinguish between waves with periods of 2 and 3 days, a total length of at  
263 least 7 days is required. This length would also be sufficient for distinguishing  
264 the diurnal tide from waves with periods of 2 days. However, it is not possible  
265 in this case to distinguish between periods of 51 and 53.3 hours. For such high  
266 spectral resolution, a length of 56 days would be required, which is longer  
267 than the duration of the wave event. Thus, the employed length of 10 days is  
268 a compromise between spectral resolution and signal smoothing. The observed  
269 wave event therefore matches the radar observations within the accuracy limits  
270 of the analysis technique.

271 Peaks at other frequencies have much less power and are likely to be associated  
272 with noise. An oscillation with a period of 2 days and eastward propagating  
273 wavenumber 2 is also found. This is very likely to be related to the eastward  
274 propagating two-day wave described by Palo et al. (2007), who found this  
275 wave to be a result of an interaction of the QTDW and the diurnal tide.

276 In order to further investigate the association of the observed wave with the  
277 mid- and low-latitude QTDW, the latitudinal extent of the wave is examined.

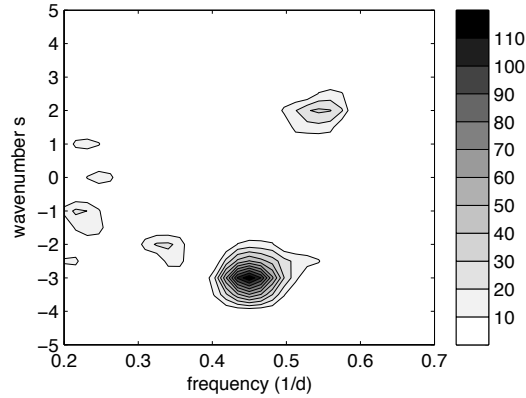


Fig. 6. Wavenumber/frequency spectrum of MLS temperature data at 0.005 hPa (86 km) and 70°S for 10 January to 31 January 2005. Positive (negative) wavenumbers denote eastward (westward) propagation.

278 The amplitude of waves with a period of 48 hours and wavenumber 3 (west-  
 279 ward) is depicted in Figure 7 as a function of latitude and time using the MLS  
 280 temperature data at 0.005 hPa (86 km). The time-series for each latitude were  
 281 smoothed with a five-day running average. Earlier it was shown that with the  
 282 MLS data it is not possible to distinguish between waves with periods close  
 283 to 2 days if window lengths less than several weeks are employed, therefore  
 284 it was not attempted to fit other periods for this analysis. A large QTDW  
 285 wave event can be observed in January and early February in the southern  
 286 hemisphere which also reaches to northern hemisphere mid-latitudes. This  
 287 large latitudinal extent has been observed previously by Limpasuvan et al.  
 288 (2005). In the northern hemisphere summer a weaker period of 2-day wave  
 289 activity is found between June and the beginning of August as expected. In  
 290 December the southern hemisphere QTDW appears again. The January and  
 291 February event at low- and mid-latitudes has been described by Limpasuvan  
 292 et al. (2005) using MLS data. It extends to 78°S, confirming that the two day  
 293 oscillations in the wind measurements over Antarctica at 68°S, 69°S, and 78°S  
 294 are likely to be associated with the well known QTDW.

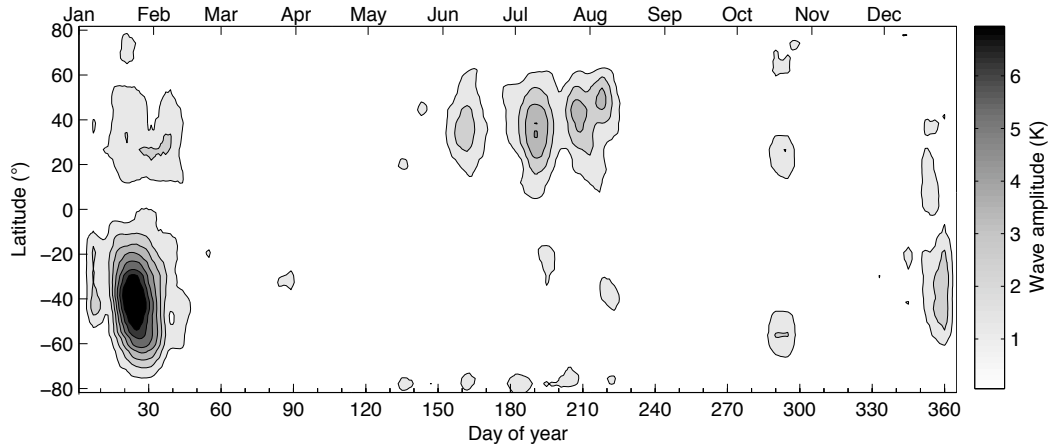


Fig. 7. Amplitude of waves with zonal wavenumber 3 (westward) and a period of 2 days as a function of latitude and day of year using MLS temperature data at 0.005 hPa (86 km) during 2005.

### 295 3.2 Wave activity in winter

296 In order to examine wave activity during winter, periodograms of the radar  
 297 wind data at 90 km (Figure 1) are compared with periodograms at 80 km  
 298 (Figure 2). At 90 km (Figure 1), in winter some wave activity is evident at  
 299 periods between two and four days. However, wave activity is stronger at lower  
 300 altitudes as seen in Figure 2. This difference in altitude between the summer  
 301 and winter 2-day oscillations has also been observed by Chshyolkova et al.  
 302 (2005) and Murphy et al. (2007). In the low frequency spectral region below  
 303 1 cyc/d, episodes of strong wave activity at various frequencies are found  
 304 between March and October. Due to differences in latitude, local influences  
 305 by gravity waves, instrumental differences, and data gaps, the similarities in  
 306 wave activity at the three sites are not strong. However, common features can  
 307 be detected. The first events in the two to four day period range are found  
 308 in May. A very short QTDW burst around 15 May is hardly discernible in  
 309 the periodograms because of its brevity but was particularly strong and is

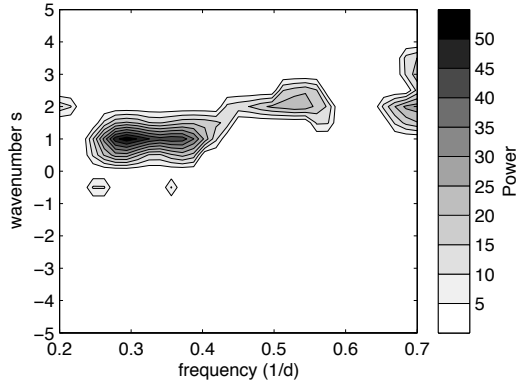


Fig. 8. Wavenumber/frequency spectrum of MLS temperature data at 0.1 hPa (64 km) and 70°S for 25 June to 9 July 2005. Positive (negative) wavenumbers denote eastward (westward) propagation.

discussed in detail in Baumgaertner et al. (2008). Wave activity in the period range of two to four days lasts until late August.

Similar to the study of the summer QTDW above, the winter waves are examined using MLS temperature data. Wavenumber/frequency analysis for a period of strong wave activity as seen in the radar data sets was performed and is shown in Figure 8. An altitude of 0.1 hPa (64 km) and a latitude of 70°S, close to the latitude of the Davis and Rothera radars, was chosen for the generation of the spectrum. The altitude is below the altitudes that can be examined by the radars, but the power in the desired frequency range was even stronger than at 80 km. Figure 8 depicts the spectrum for 25 June to 9 July 2005. Power is distributed over a range of frequencies and wavenumbers. A QTDW wave with wavenumber 2 is evident, but there are also strong 3-day and 4-day oscillations with zonal wavenumber 1.

The combined appearance of several waves with similar phase speeds has in the past led to the suggestion that the waves are quasi-non-dispersive. When

325 several non-dispersive waves with small wavenumbers circle the pole at the  
326 same velocity, strong temperature maxima occur which have been termed  
327 “warm pools” (Prata, 1984). They can be directly observed in MLS tempera-  
328 ture maps during several periods. As an example, Figure 9 depicts interpolated  
329 ( $2^\circ$  latitude and  $10^\circ$  longitude grid) temperature maps at 0.3 hPa (57 km) for  
330 5–7 August 2005 in intervals of 12 hours. The blue crosses mark the temper-  
331 ature maxima. The warmest region in Figure 9a is located at approximately  
332  $0^\circ$  longitude and moves eastward until it reaches  $90^\circ$ W in the last map of the  
333 sequence, Figure 9f. The average velocity of the warm pool is therefore about  
334  $90^\circ$  longitude per day, which can be described as a wavenumber 1 wave with a  
335 period of four days. Note the presence of a secondary temperature maximum  
336 located on the opposite side of the pole. In combination with the primary  
337 maximum, this leads to a wavenumber 2 wave with a period of 2 days.

338 The behavior of the primary maximum is further studied by analysing its po-  
339 sition as a function of time for the entire winter of 2005. This is depicted in  
340 Figure 10 where the unwrapped longitude of the temperature maximum at  
341 0.3 hPa was determined on 12 hourly temperature maps of the area south of  
342  $40^\circ$ S (similar to the blue crosses in Figure 9). There is little consistent zonal  
343 movement before day 200 (19 July), but after that date the temperature max-  
344 imum rotates around the pole at a constant angular velocity of approximately  
345 4 to 4.5 days per rotation. This feature exists for about 1 month. These find-  
346 ings agree well with previous observations related to warm pools and their  
347 phase velocities (e.g. Lawrence et al., 1995).

348 The 2- and 4-day temperature oscillations are further discussed by analysing  
349 their behavior as a function of altitude and time of year. The average wave  
350 amplitudes of the eastward propagating 2-day wave with zonal wavenumber 2

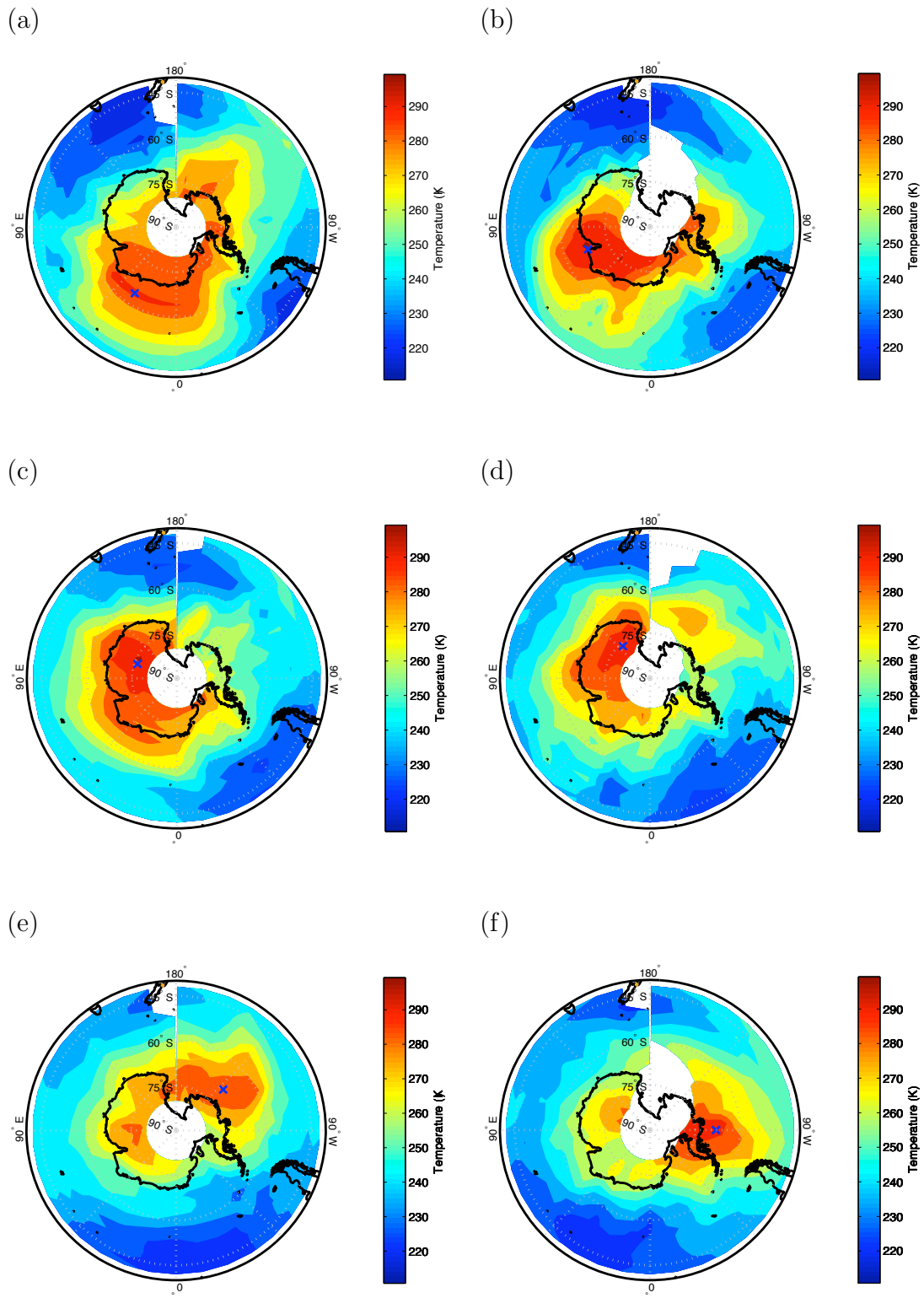


Fig. 9. 12-hourly temperature maps for 0.3 hPa (57 km) obtained by MLS for 5–7 August 2005.

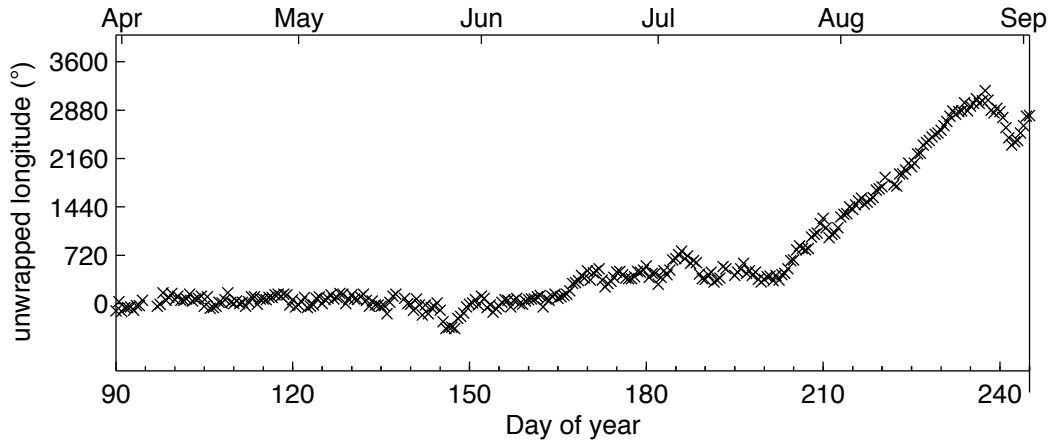


Fig. 10. Unwrapped longitude of the maximum on 12-hourly interpolated temperature maps at 0.3 hPa during winter 2005.

351 and the 4-day wave with zonal wavenumber 1 between 60°S and 70°S is shown  
 352 in Figure 11. Periods of strong wave activity are noted in June as well as late  
 353 July/early August in the upper stratosphere and mesosphere with maximum  
 354 amplitudes of 4.5 K. In the mesosphere, smaller amplitude waves occur until  
 355 September. In the stratosphere the wave moves towards lower altitudes in time  
 356 until late October. When this average amplitude is compared to the individual  
 357 amplitudes of the 2- and 4-day wave (not shown), it is evident that the mean  
 358 amplitude of the two waves is less variable than the individual amplitudes  
 359 throughout the southern hemisphere winter. At 70°S and 50 km altitude for  
 360 example, the coefficient of variation for the average wave activity is 36%,  
 361 compared with 63% for the two-day wave and 48% for the four-day wave. This  
 362 could be interpreted as the presence of a source of wave forcing which leads to  
 363 the 4-day and 2-day wave depending on other unknown factors. A potential  
 364 candidate for such a constant source is the polar night jet which can create  
 365 shear instabilities. This has previously been pointed out by Plumb (1983).  
 366 Since then, planetary waves in the stratosphere and mesosphere with periods  
 367 between two and four days have been successfully reproduced in mechanistic

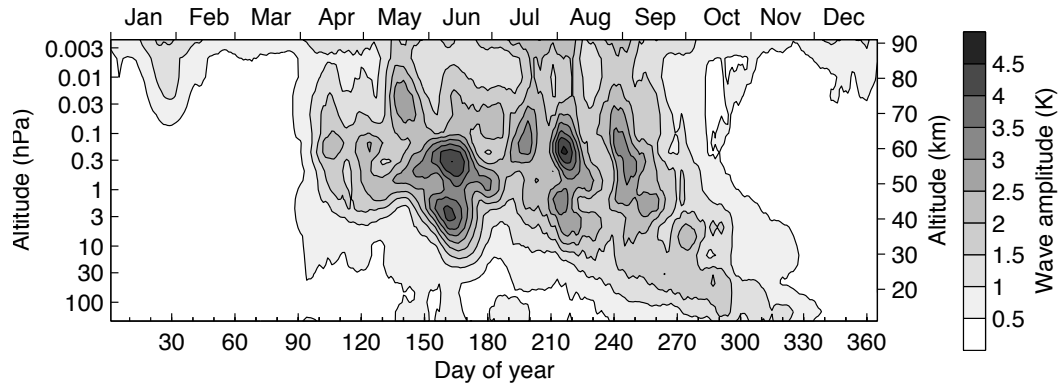


Fig. 11. Average of the MLS temperature amplitudes of the 2-day and 4-day wave with wavenumbers 2 and 1, respectively between 60°S and 70°S for the year 2005.

368 and general circulation models. These studies indicate that baroclinic and  
 369 barotropic instabilities are important for the generation of this type of wave.  
 370 The baroclinic and barotropic instabilities are related to the polar night jet.  
 371 For both types of instabilities the part of the time-dependence that depends  
 372 on the strength of the jet are similar. However, the variation of the horizontal  
 373 and vertical location of the jet will influence the baroclinic and barotropic  
 374 instabilities in a different way. Therefore, distinguishing between the two types  
 375 of instabilities in the data is possible.

376 It is first determined whether there is a relationship between the strength of  
 377 the winter stratospheric jet and wave activity as instabilities are more likely  
 378 to be created by high wind velocities. The zonal wind velocity taken from  
 379 the UKMO assimilation averaged over 60°S and 70°S is shown in Figure 12.  
 380 There is qualitative agreement between the wind velocity and wave activity  
 381 (Figure 11). For example, strong winds in June as well as in late July and  
 382 early August at 40 km and between 40 and 60 km, respectively, correspond  
 383 well to enhancements in wave activity at corresponding locations in time and

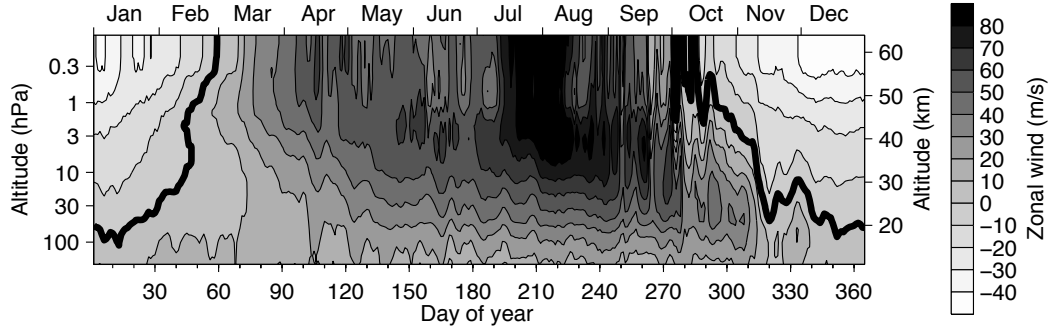


Fig. 12. Average zonal wind velocity between 60°S and 70°S derived from the UKMO assimilation. The bold line indicates the zero-wind line.

384 altitude.

385 We now examine the relative importance of the baroclinic and barotropic  
386 instabilities separately.

387 Baroclinic instabilities are associated with the vertical shear of the zonal wind,  
388 whereas barotropic instabilities arise from the horizontal shear of the zonal  
389 wind. The vertical shear can be approximated through the thermal wind shear  
390 balance equation (Andrews, 2000):

$$391 \quad -\frac{g}{T} \frac{\partial T}{\partial y} = f \frac{\partial u}{\partial z} \quad (3)$$

392 where  $\partial T/\partial y$  is temperature gradient in the meridional direction,  $u$  is the  
393 zonal wind,  $z$  is altitude,  $f$  is the Coriolis parameter, and  $g$  is the acceleration  
394 due to gravity.

395 Due to the high inclination of the Aura satellite, the temperature measure-  
396 ments of the MLS instrument are performed along circles of constant longi-  
397 tude to a reasonably good approximation, although this does not hold true  
398 in the vicinity of the pole. Therefore, the latitudinal temperature gradient

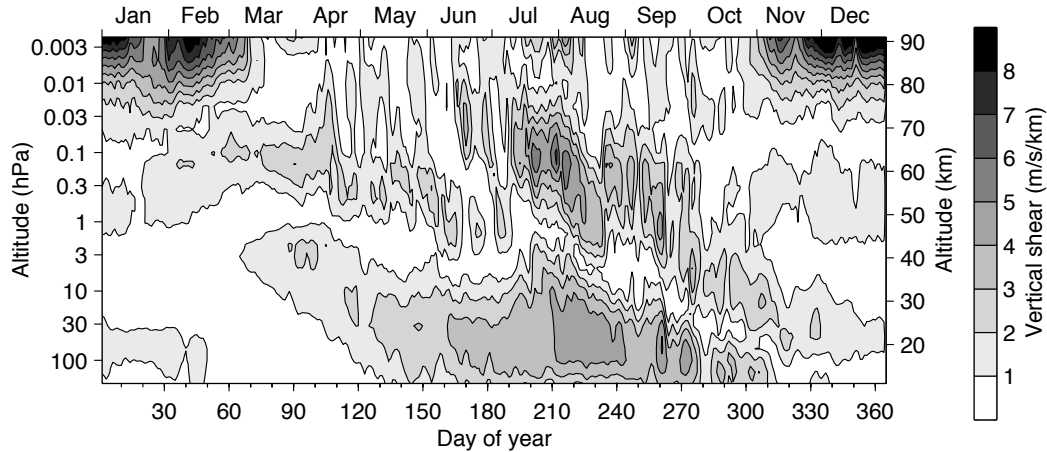


Fig. 13. Average vertical wind shear between 60°S and 70°S during 2005, derived from MLS temperature measurements.

399 can be computed from consecutive measurements from each orbit up to ap-  
 400 proximately 70° latitude. The vertical wind shear is easily computed using  
 401 equation 3. The derived wind shear was averaged over all longitudes, there-  
 402 fore encompassing several orbits, and over 60°S to 70°S. This procedure is  
 403 likely to filter out local instabilities due to gravity waves for example. The  
 404 resulting mean wind shear is depicted in Figure 13. Strong shear is observed  
 405 during summer above 75 km, and in winter shear is found throughout the  
 406 stratosphere and mesosphere below 70 km with a gap at about 40 km which  
 407 is the altitude where the jet maximises (Hibbins et al., 2005). Hibbins et al.  
 408 (2005) studied the mean wind field at Rothera (68°S) and found that the  
 409 summer mesospheric jet maximized at 65 km, the winter jet had maximum  
 410 velocities at 40 km, in good agreement with the data presented in Figure 12.  
 411 Strong vertical shear was observed in the altitude regions up to 20 km above  
 412 the jets. This is confirmed by the MLS vertical wind shear data in Figure 13.  
 413 The wind shear at upper levels is generally attributed to gravity wave mo-  
 414 mentum deposition accompanying wave dissipation processes.

415 The observed shear has the potential to cause baroclinic instabilities which  
416 can create planetary scale waves by releasing potential energy. The vertical  
417 shear is related to baroclinity  $b$ , which is defined as:

$$418 \quad b = \frac{1}{P} \frac{\partial P}{\partial \phi} - \frac{1}{\rho} \frac{\partial \rho}{\partial \phi} \quad (4)$$

419 where  $P$  is pressure,  $\rho$  is density, and  $\phi$  is latitude. Using the ideal gas  
420 law it can be shown that:

$$421 \quad b = \frac{1}{T} \frac{\partial T}{\partial \phi} \quad (5)$$

422 From equation 3 it follows that  $\partial u / \partial z \propto b$ . It can be shown that a baroclinic  
423 atmosphere can release potential energy and develop instabilities (Andrews,  
424 2000). Therefore, a relationship between wave activity and shear would be ex-  
425 pected.

426 During summer, the strong shear between 80 and 90 km corresponds well with  
427 the time and altitude where wave activity was observed in the radar and tem-  
428 perature data (e.g. Figure 4). Comparison of the time and altitude behavior of  
429 the winter planetary waves (Figures 11) with the observed shear (Figure 13)  
430 shows that a similar pattern is also observed. For example, the burst of wave  
431 activity in late July and early August discussed earlier corresponds well to  
432 an enhancement in vertical shear. It should be noted that the similarities are  
433 greater at 60°S, where the shear is also larger in general, than at 70°S (not  
434 shown). The relationship can be further examined by studying the correla-  
435 tion between wave activity and vertical shear. As for the computation of the  
436 data for Figure 11, the mean amplitude of waves with periods of two and four  
437 days and zonal wavenumbers 2 and 1, respectively, was chosen as a measure

438 of wave activity. The correlation coefficient was only computed for the pe-  
439 riod from June to September in order to avoid contamination by the seasonal  
440 variation. The Pearson correlation coefficient is only valid if the probability  
441 distribution is normal, but if the seasonal variation was included, the distribu-  
442 tion of values would not be normal. The correlation is strongly dependent on  
443 the altitude and latitude region examined. Here we present results from 60°S  
444 and 70°S. At 60°S the correlation is significant above the 95% level between  
445 60 and 70 km altitude, the correlation coefficient reaches 0.6. At 70°S, the  
446 correlation was not found to be significant. Note that introducing time lags  
447 between the two quantities did not improve the results. It has to be kept in  
448 mind that a linear relationship between baroclinity and wave activity would  
449 not necessarily be expected. In addition, the temporal and spatial distribution  
450 of waves is unlikely to be represented accurately by the measurements, nor will  
451 the analysis technique of summing a 2- and 4-day wave always be the correct  
452 technique. For these reasons, the presented analysis remains mostly qualita-  
453 tive. However, a more thorough theoretical and experimental approach might  
454 enable a more quantitative understanding, which is unfortunately beyond the  
455 scope of this work.

456 It has also been shown that barotropic instabilities have the ability to create  
457 short-period planetary waves (e.g. Hartmann, 1983). It is not possible to infer  
458 the latitudinal shear of the zonal wind from MLS measurements, therefore the  
459 UKMO assimilated data are used to approximate this parameter. However,  
460 the upper boundary of the UKMO data is at 0.1 hPa and therefore the wave  
461 activity period in summer, which occurs above that altitude, cannot be ex-  
462 amined with this data set. The horizontal shear as a function of altitude and  
463 time in 2005, derived as the latitudinal gradient of the zonal wind, is shown for

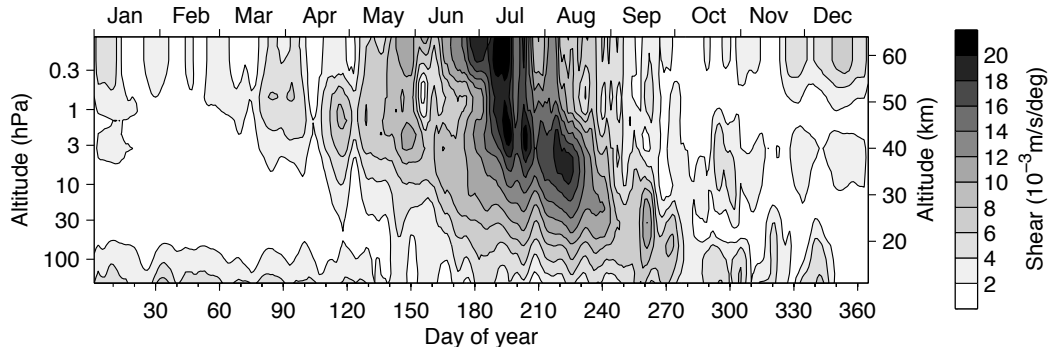


Fig. 14. Horizontal wind shear at 70°S during 2005, derived from UKMO zonal wind data.

464 70°S in Figure 14. The correspondence between horizontal shear (Figure 14)  
 465 and wave activity (Figure 11) is similarly good as for the case of vertical shear  
 466 and wave activity. The largest shear is observed in July and early August,  
 467 corresponding to the high wind velocities that were discussed earlier during  
 468 that time, and thus also corresponds to wave activity.

469 Similar to the analysis of the relationship between baroclinity and wave ac-  
 470 tivity, the correlation coefficients were calculated for wave activity and the  
 471 horizontal wind shear at 60°S and 70°S. At 60°S no significant correlation was  
 472 evident, but at 70°S the correlation was significant and reached approximately  
 473 0.5 at 60 km altitude. Again it has to be stressed that due to the measurements  
 474 and the analysis technique such quantitative analysis must remain tentative.  
 475 Here, the limitations are even stronger since the MLS measurements are com-  
 476 pared to the UKMO assimilation.

477 Summarising the results from the shear analysis despite the limitations on  
 478 the analysis presented, we conclude that both horizontal and vertical shear  
 479 appear to be related to wave activity as expected since they are both related  
 480 to the strength of the jet. However, wave activity relates most strongly to

481 the dominant type of shear in the latitudinal region examined. This is physi-  
482 cally sensible and indicates that the above described mechanisms of instabil-  
483 ity generation through shear contribute significantly to wave activity in the  
484 stratosphere and mesosphere.

## 485 4 Conclusions

486 MFSA radar wind measurements at Scott Base, Rothera, and Davis showed  
487 an oscillation with a period of approximately two days during late January  
488 and early February 2005. The amplitude of the oscillation maximises at about  
489 90 km altitude and was found to have a westward propagating zonal wavenum-  
490 ber 3 structure which indicates a relationship to the QTDW commonly ob-  
491 served at low- and mid-latitudes. Satellite measurements of the latitudinal  
492 extent confirm this conclusion. The Scott Base measurements of the QTDW  
493 appear to be the highest-latitude observations of the QTDW published.

494 In winter, oscillations with periods between two and four days are promi-  
495 nent with maximum amplitudes below 80 km. These waves were found to be  
496 eastward propagating and to have zonal wavenumbers of 1 and 2. The MLS  
497 temperature data showed that when several waves with different periods occur  
498 at the same time, they often have similar phase velocities, supporting sugges-  
499 tions that they are quasi-non-dispersive. Such a “warm pool” was observed by  
500 MLS from late July to late August 2005. The observations showed that the  
501 average wave activity, computed as the mean of the two- and four-day oscilla-  
502 tions, is more constant than the activity of the individual waves. This can be  
503 interpreted as the existence of a relatively constant wave-forcing mechanism  
504 such as shear instabilities which are related to the polar night jet. Vertical and

505 horizontal shear of the zonal wind, which can create baroclinic and barotropic  
506 instabilities, respectively, were studied using satellite and assimilated data in  
507 order to determine if a relationship to wave activity exists. The results indi-  
508 cated that vertical shear, which is larger at 60°S than at 70°S, contributes  
509 more to wave activity at 60°S. The opposite is true for the horizontal shear,  
510 which is largest at 70°S and appears to contribute more to wave activity there  
511 than vertical shear. However, the disadvantages of the measurements and the  
512 analysis were discussed and found to limit the conclusions that can be drawn.  
513 Additional analysis involving potential vorticity to assess instability potential  
514 and expected linear growth rates could further quantify the obtained results.

## 515 **Acknowledgements**

Some of this work was carried out at the British Antarctic Survey (BAS) which was made possible by funding from BAS and the University of Canterbury Department of Physics and Astronomy. Work to ensure operation of the radars carried out by the technical staff at the University of Canterbury, BAS, and at the three bases in Antarctica is acknowledged. Logistic support for the Scott Base MFSA radar was provided by Antarctica New Zealand. Operational and research activities associated with the Davis MF radar have been supported by Australian Antarctic Science Advisory Committee grant number 674. The Rothera MF radar is a joint collaboration between BAS and NorthWest Research Associates/Colorado Research Associates Division, funded by NSF through grant #ATM 0438777 and the UK Natural Environment Research Council. The EOS MLS data were provided by the Jet Propulsion Laboratory/NASA via their website. The United Kingdom Met. Office

stratospheric assimilated data (UKMO) were made available by the British Atmospheric Data Centre.

## 516 **References**

- 517 Andrews, D. G., 2000. An Introduction to Atmospheric Physics. Cambridge  
518 University Press, Cambridge.
- 519 Andrews, D. G., Holton, J. R., Leovy, C. B., 1987. Middle atmosphere dy-  
520 namics. International geophysics series ; v. 40. Academic Press, Orlando.
- 521 Baumgaertner, A. J. B., McDonald, A. J., Jöckel, P., Brühl, C., Murphy,  
522 D. J., 2008. Observations and CCM modelling of a planetary wave burst:  
523 Connections to a solar proton event? JASTP, in preparation.
- 524 Baumgaertner, A. J. G., Jarvis, M. J., McDonald, A. J., Fraser, G. J., 2006.  
525 Observations of the wavenumber 1 and 2 components of the semi-diurnal  
526 tide over Antarctica. *Journal of Atmospheric and Solar-Terrestrial Physics*  
527 68 (11), 1195–1214.
- 528 Baumgaertner, A. J. G., McDonald, A. J., 2007. A gravity wave climatology  
529 for Antarctica compiled from Challenging Minisatellite Payload/Global Po-  
530 sitioning System (CHAMP/GPS) radio occultations. *Journal of Geophysical*  
531 *Research (Atmospheres)* 112, D05103, doi:10.1029/2006JD007504.
- 532 Baumgaertner, A. J. G., McDonald, A. J., Fraser, G. J., Plank, G. E., 2005.  
533 Long-term observations of mean winds and tides in the upper mesosphere  
534 and lower thermosphere above Scott Base, Antarctica. *Journal of Atmo-*  
535 *spheric and Solar-Terrestrial Physics* 67 (16), 1480–1496.
- 536 Charney, J. G., Stern, M. E., 1962. On the Stability of Internal Baroclinic  
537 Jets in a Rotating Atmosphere. *Journal of the Atmospheric Sciences* 19 (2),  
538 159–172.

539 Chshyolkova, T., Manson, A. H., Meek, C. E., 2005. Climatology of the quasi  
540 two-day wave over Saskatoon (52 degrees N, 107 degrees W): 14 Years of  
541 MF radar observations. *Advances in Space Research* 35 (11), 2011–2016.

542 Craig, R. L., Elford, W. G., 1981. Observations of the Quasi 2-Day Wave near  
543 90 Km Altitude at Adelaide (35°S). *Journal of Atmospheric and Terrestrial*  
544 *Physics* 43 (10), 1051–1056.

545 Fraser, G. J., Hernandez, G., Smith, R. W., 1993. Eastward-Moving 2-4 Day  
546 Waves in the Winter Antarctic Mesosphere. *Geophysical Research Letters*  
547 20 (15), 1547–1550.

548 Fritts, D. C., Isler, J. R., Lieberman, R. S., Burrage, M. D., Marsh, D. R.,  
549 Nakamura, T. K., Tsuda, T., Vincent, R. A., 1999. Two-day wave structure  
550 and mean flow interactions observed by radar and High Resolution Doppler  
551 Imager. *Journal of Geophysical Research* 104 (D4), 3953–3969.

552 Fritts, D. C., Vincent, R. A., 1987. Mesospheric Momentum Flux Studies at  
553 Adelaide, Australia - Observations and a Gravity Wave-Tidal Interaction-  
554 Model. *Journal of the Atmospheric Sciences* 44 (3), 605–619.

555 Froidevaux, L., Livesey, N. J., Read, W. G., Jiang, Y. B. B., Jimenez, C.,  
556 Filipiak, M. J., Schwartz, M. J., Santee, M. L., Pumphrey, H. C., Jiang,  
557 J. H., Wu, D. L., Manney, G. L., Drouin, B. J., Waters, J. W., Fetzer, E. J.,  
558 Bernath, P. F., Boone, C. D., Walker, K. A., Jucks, K. W., Toon, G. C.,  
559 Margitan, J. J., Sen, B., Webster, C. R., Christensen, L. E., Elkins, J. W.,  
560 Atlas, E., Lueb, R. A., Hendershot, R., 2006. Early validation analyses of  
561 atmospheric profiles from EOS MLS on the Aura satellite. *Ieee Transactions*  
562 *on Geoscience and Remote Sensing* 44 (5), 1106–1121.

563 Garcia, R. R., Lieberman, R., Russell, J. M., Mlynczak, M. G., 2005. Large-  
564 scale waves in the mesosphere and lower thermosphere observed by SABER.

565 Journal of the Atmospheric Sciences 62 (12), 4384–4399.

566 Glass, M., Fellous, J. L., Masseur, M., Spizzichino, A., Lysenko, I. A., Port-  
567 niaghin, Y. I., 1975. Comparison and Interpretation of Results of Simulta-  
568 neous Wind Measurements in Lower Thermosphere at Garchy (France) and  
569 Obninsk (USSR) by Meteor Radar Technique. *Journal of Atmospheric and*  
570 *Terrestrial Physics* 37 (8), 1077–1087.

571 Harris, T. J., 1994. A Long-Term Study of the Quasi-2-Day Wave in the Middle  
572 Atmosphere. *Journal of Atmospheric and Terrestrial Physics* 56 (5), 569–  
573 579.

574 Hartmann, D. L., 1983. Barotropic Instability of the Polar Night Jet-Stream.  
575 *Journal of the Atmospheric Sciences* 40 (4), 817–835.

576 Hibbins, R. E., Shanklin, J. D., Espy, P. J., Jarvis, M. J., Riggin, D. M.,  
577 Fritts, D. C., Lübken, F.-J., 2005. Seasonal variations in the horizontal wind  
578 structure from 0-100 km above Rothera station, Antarctica (67°S, 68°W).  
579 *Atmospheric Chemistry and Physics* 5, 2973–2980.

580 Jarvis, M. J., Jones, G. O. L., Jenkins, B., 1999. New initiatives in observing  
581 the Antarctic mesosphere. *Advances in Space Research* 24 (5), 611–619.

582 Kalchenko, B. V., Bulgakov, S. V., 1973. Study of periodic components of  
583 wind velocity in the lower thermosphere above the equator. *Geomagnetism*  
584 *and Aeronomy (Translation)* 13 (955-956).

585 Lawrence, B. N., Fraser, G. J., Vincent, R. A., Phillips, A., 1995. The 4-  
586 Day Wave in the Antarctic Mesosphere. *Journal of Geophysical Research*  
587 100 (D9), 18899–18908.

588 Limpasuvan, V., Wu, D. L., 2003. Two-day wave observations of UARS Mi-  
589 crowave Limb Sounder mesospheric water vapor and temperature. *Journal*  
590 *of Geophysical Research* 108 (D10), doi:10.1029/2002JD002903.

591 Limpasuvan, V., Wu, D. L., Schwartz, M. J., Waters, J. W., Wu, Q., Killeen,

592 T. L., 2005. The two-day wave in EOS MLS temperature and wind mea-  
593 surements during 2004-2005 winter. *Geophysical Research Letters* 32 (17),  
594 doi:10.1029/2005GL023396.

595 Manney, G. L., 1991. The Stratospheric 4-Day Wave in NMC Data. *Journal*  
596 *of the Atmospheric Sciences* 48 (15), 1798–1811.

597 Manney, G. L., Nathan, T. R., Stanford, J. L., 1988. Barotropic Stability of  
598 Realistic Stratospheric Jets. *Journal of the Atmospheric Sciences* 45 (18),  
599 2545–2555.

600 Meek, C. E., Manson, A. H., Franke, S. J., Singer, W., Hoffmann, P., Clark,  
601 R. R., Tsuda, T., Nakamura, T., Tsutsumi, M., Hagan, M., Fritts, D. C.,  
602 Isler, J., Portnyagin, Y. I., 1996. Global study of northern hemisphere quasi-  
603 2-day wave events in recent summers near 90 km altitude. *Journal of At-*  
604 *mospheric and Terrestrial Physics* 58 (13), 1401–1411.

605 Muller, H. G., 1972. Long-Period Meteor Wind Oscillations. *Philosophical*  
606 *Transactions of the Royal Society of London Series a-Mathematical and*  
607 *Physical Sciences* 271 (1217), 585–599.

608 Murphy, D. J., 2002. Variations in the phase of the semidiurnal tide over Davis,  
609 Antarctica. *Journal of Atmospheric and Solar-Terrestrial Physics* 64 (8-11),  
610 1069–1081.

611 Murphy, D. J., French, W. J. R., Vincent, R. A., 2007. Long-Period  
612 Planetary Waves in the mesosphere and lower thermosphere above  
613 Davis, Antarctica. *Journal of Atmospheric and Solar-Terrestrial Physics*,  
614 doi:10.1016/j.jastp.2007.06.008.

615 Norton, W. A., Thuburn, J., 1996. The two-day wave in a middle atmosphere  
616 GCM. *Geophysical Research Letters* 23 (16), 2113–2116.

617 Nozawa, S., Imaida, S., Brekke, A., Hall, C. M., Manson, A., Meek, C.,  
618 Oyama, S., Dobashi, K., Fujii, R., 2003a. The quasi 2-day wave observed

619 in the polar mesosphere. *Journal of Geophysical Research* 108 (D2), 4039,  
620 doi:10.1029/2002JD002440.

621 Nozawa, S., Iwahashi, H., Brekke, A., Hall, C. M., Meek, C., Manson, A.,  
622 Oyama, S., Murayama, Y., Fujii, R., 2003b. The quasi 2-day wave ob-  
623 served in the polar mesosphere: Comparison of the characteristics observed  
624 at Tromso and Poker Flat. *Journal of Geophysical Research* 108 (D24),  
625 4748, doi:10.1029/2002JD003221.

626 Palo, S. E., Forbes, J. M., Zhang, X., Russell, J. M., Mlynczak, M. G., 2007. An  
627 eastward propagating two-day wave: Evidence for nonlinear planetary wave  
628 and tidal coupling in the mesosphere and lower thermosphere. *Geophysical*  
629 *Research Letters* 34, L07807, doi:10.1029/2006GL027728.

630 Palo, S. E., Portnyagin, Y. I., Forbes, J. M., Makarov, N. A., Merzlyakov,  
631 E. G., 1998. Transient eastward-propagating long-period waves observed  
632 over the South Pole. *Annales Geophysicae* 16, 1486–1500.

633 Pfister, L., 1985. Baroclinic Instability of Easterly Jets with Applications to  
634 the Summer Mesosphere. *Journal of the Atmospheric Sciences* 42 (4), 313–  
635 330.

636 Plumb, R. A., 1983. Baroclinic Instability of the Summer Mesosphere: a Mech-  
637 anism for the Quasi-Two-Day Wave? *Journal of the Atmospheric Sciences*  
638 40 (1), 262–270.

639 Prata, A. J., 1984. The 4-Day Wave. *Journal of the Atmospheric Sciences*  
640 41 (1), 150–155.

641 Randel, W. J., 1994. Observations of the 2-Day Wave in NMC Stratospheric  
642 Analyses. *Journal of the Atmospheric Sciences* 51 (2), 306–313.

643 Randel, W. J., Lait, L. R., 1991. Dynamics of the 4-Day Wave in the  
644 Southern-Hemisphere Polar Stratosphere. *Journal of the Atmospheric Sci-*

645 ences 48 (23), 2496–2508.

646 Rodgers, C. D., Prata, A. J., 1981. Evidence for a Traveling 2-Day Wave in  
647 the Middle Atmosphere. *Journal of Geophysical Research* 86 (NC10), 9661–  
648 9664.

649 Salby, M. L., 1981. The 2-Day Wave in the Middle Atmosphere: Observations  
650 and Theory. *Journal of Geophysical Research* 86 (NC10), 9654–9660.

651 Salby, M. L., 1984. Survey of Planetary-Scale Traveling Waves - the State of  
652 Theory and Observations. *Reviews of Geophysics* 22 (2), 209–236.

653 Swinbank, R., Lahoz, W. A., O’Neill, A., Douglas, C. S., Heaps, A., Podd, D.,  
654 1998. Middle atmosphere variability in the UK Meteorological Office Unified  
655 Model. *Quarterly Journal of the Royal Meteorological Society* 124 (549),  
656 1485–1525.

657 Torrence, C., Compo, G. P., 1998. A practical guide to wavelet analysis. *Bul-*  
658 *letin of the American Meteorological Society* 79 (1), 61–78.

659 Venne, D. E., Stanford, J. L., 1979. Observation of a 4-Day Temperature  
660 Wave in the Polar Winter Stratosphere. *Journal of the Atmospheric Sciences*  
661 36 (10), 2016–2019.

662 Volland, H., 1988. Atmospheric tidal and planetary waves. Atmospheric sci-  
663 ences library. Kluwer Academic Publishers ; Sold and distributed in the  
664 U.S.A. and Canada by Kluwer Academic Publishers, Dordrecht ; Boston  
665 Norwell, MA, U.S.A.

666 Wu, D. L., Hays, P. B., Skinner, W. R., 1995. A Least-Squares Method for  
667 Spectral-Analysis of Space-Time Series. *Journal of the Atmospheric Sciences*  
668 52 (20), 3501–3511.

669 Wu, D. L., Hays, P. B., Skinner, W. R., Marshall, A. R., Burrage, M. D.,  
670 Lieberman, R. S., Ortland, D. A., 1993. Observations of the Quasi 2-Day  
671 Wave from the High-Resolution Doppler Imager on UARS. *Geophysical Re-*

672 search Letters 20 (24), 2853–2856.